ARTICLE TYPE

Anisotropic wave propagation in nematic liquid crystals

Paolo Biscari,[a] **Antonio DiCarlo,**[b] **and Stefano S. Turzi** [*a]

Despite the fact that quantitative experimental data have been available for more than forty years now, nematoacoustics still poses intriguing theoretical and experimental problems. In this paper, we prove that the main observed features of acoustic wave propagation through a nematic liquid crystal cell – namely, the frequency-dependent anisotropy of sound velocity and acoustic attenuation – can be explained by properly accounting for two fundamental features of the nematic response: *anisotropy* and *relaxation*. The latter concept – new in liquid crystal modelling – provides the first theoretical explanation of the structural relaxation process hypothesised long ago by Mullen and co-workers [Mullen et al., *Phys. Rev. Lett.*, 1972, **28**, 799]. We compare and contrast our proposal with an alternative theory where the liquid crystal is modelled as an anisotropic second-gradient fluid.

1 Introduction

Nematic liquid crystals (NLCs from now on) are anisotropic elastic fluids whose symmetry axis – the nematic *director* – depends on the prevailing molecular orientation. The quadrupolar character of most NLCs extends their anisotropic response to the electric and magnetic susceptibilities, making thus possible to strongly manipulate their orientational pattern with negligible accompanying deformations. Based on this observation, the early Oseen-Frank theory[1,2] considered the orientational response of NLCs completely decoupled from their macroscopic motion. The variational continuum theory that emerged from it by accounting properly for the nematic symmetry satisfactorily predicts the equilibrium behaviour of NLCs – at least far from the nematic-isotropic transition and away from defects. The best-established dynamical extension of the Oseen-Frank theory, originally put forward by Ericksen[3] and fully developed by Leslie[4], while allowing for the (linear) effects of nematic anisotropy on the viscous response, does not cover the experimentally observed effects of the (slight) compressibility of NLCs.

In fact, it has long been recognised that sound waves interact with the orientational order of NCLs, often in a rather subtle way[5]. For instance, strong sound waves impinging on an NLC cell have been observed to induce shear flows which, in turn, perturb the nematic alignment. But also in the linear acoustic regime a variety of interesting effects have been detected. A low intensity ultrasonic wave injected into an NLC cell changes its optical transmission properties, namely, its re-

fractive index. Even in Fermi liquids the onset of nematic order dramatically affects the behaviour of sound waves[6]. Recently, this acousto-optic effect has attracted renewed attention, due to its potential for application to acoustic imaging[7,8]. A different manifestation of the coupling between acoustic waves and nematic order is the phenomenon of acoustic generation observed in an NLC cell undergoing Fréedericksz transitions triggered by an external electric field[9].

In the following, we specifically focus on the anisotropic propagation of acoustic waves through an NLC cell where the mass density and the nematic field are uniform in the unperturbed state. This phenomenon was studied experimentally more than forty years ago by Mullen, Lüthi and Stephen[10]. They found that the speed of sound is maximum when the direction of propagation is along the nematic director and minimum when it is orthogonal to it. The difference is minimal – a few thousandths of the average sound speed – and exhibits a peculiar dependence on the sound frequency, while being roughly independent of temperature in the considered range.

That most remarkable experimental paper provides also some valuable hints at a plausible theoretical explanation. To our present purposes, this is the key quote from Ref. 10: 'The experimental anisotropy in the sound velocity indicates that at finite frequencies a liquid crystal has an anisotropic compressibility. This anisotropy can be explained if at these frequencies a liquid crystal in some respects behaves like a solid[*] . . . However, the elastic constants must have an important frequency dependence . . . If this were not the case, it would cost a finite energy to change the shape of a liquid crystal, the volume being kept constant. This is not consistent with our present ideas of the structure of a liquid crystal. The frequency dependence

[a] *Dipartimento di Matematica, Politecnico di Milano, Piazza Leonardo da Vinci, 32   20133 Milano, Italy*
[b] *Dipartimento di Matematica & Fisica, Università Roma Tre, Via della Vasca Navale, 84   00146 Roma, Italy*
[*] *E-mail: stefano.turzi@polimi.it*

[*] The specific free energy conjectured in Ref. 10, omitted in this introductory quote, is reported literatim as (B.19) in Appendix B, where it is related to the one we put forth in Sec.2.

of the elastic constants could arise out of some structural relaxation process in the liquid crystal.'

In this paper, building on the experimental results and the theoretical conjectures of Mullen, Lüthi and Stephen[10], we construct a complete theory consistent with their observations, based on two main hypotheses: first, the elastic response to expansion/rarefaction strains is assumed to be affected by the nematic order; second, the structural processes characterising the fluidity of NLCs are modelled by introducing an evolving relaxed configuration[11,12].

To explain the same effects, a different line of thought was followed by Selinger and co-workers, who postulated that the sound-speed anisotropy is due to a direct coupling between the nematic director and the spatial gradient of the mass density[13–16]. This idea was subsequently fully developed into a theory of anisotropic Korteweg-like fluids by Virga[17]. Because of mass conservation, the mass density is related to the determinant of the strain. Therefore, the Selinger-Virga hypothesis establishes a *second-gradient* theory, i.e., an elastic theory where the strain energy depends also on the second derivatives of the displacement. Since higher-gradient terms compete with the standard first-gradient terms, they typically represent singular perturbations to the underlying first-gradient theory. Accordingly, their contribution becomes important only if and where abrupt density changes take place. In fact, the original proposal by Korteweg was meant to model interfacial and capillary forces by resolving density discontinuities into smooth but steep density variations[18]. It seems therefore implausible that the mild density undulations occurring in the linear acoustic regime may produce sizeable second-gradient effects.

This work is organised as follows. Sec. 2 is devoted to the introduction of an elastic strain energy properly accounting for nematic anisotropy. In Sec. 2.1 we show preliminarily that the elastic response included in the early visco-elastic assumption put forward by Ericksen in his seminal work on anisotropic fluids[3] suffices to produce an anisotropic (frequency independent) speed of sound. However, we also prove that such an assumption is incompatible with anisotropic hyperelasticity. We then proceed to construct a stored energy density function capable of representing the elastic behaviour of slightly compressible NLCs (Secs. 2.2 and 2.3). On this basis, in Sec. 2.4 a perturbation analysis is used to obtain a satisfactory dependence of the speed of sound on the angle between the wave vector and the nematic director. In Sec. 3 we introduce and exploit the crucial concept of nematic relaxation, a mechanism allowing the shear stress to relax (with a characteristic time typically much smaller than the director relaxation time). The equation governing the evolution of the relaxed configuration is given in Sec. 3.1. The frequency dependence of the speed and attenuation of sound waves is obtained in Sec. 3.2. Sec. 4 contains a discussion, where our theoretical predictions

are tested against experimental data. The results we obtain compare well with the experimental findings by Mullen, Lüthi and Stephen[10] and other early authors[19]. Further developments are finally pointed out. Two appendices complete the paper. In Appendix A we prove that Ericksen's early constitutive assumption for the Cauchy stress in an anisotropic elastic fluid cannot be hyperelastic. Appendix B, besides collecting several computational details of our nonlinear nematic hyperelastic theory, presents a thorough comparison of its linearised version and the small-displacement theory hinted at by Mullen et al.[10].

2 Nematic elasticity

Isothermal conditions are assumed in all what follows. Moreover, we assume that the NLC, uniformly aligned in its unperturbed state, stays so while traversed by the acoustic wave. These assumptions reflect the setup of all the cited experimental studies[†]. To get an idea of the (small) effects of the removal of the constraint on the nematic texture, see Refs. 20, 21. To stress that the director field is uniform and stationary, we shall denote it by $\mathbf{n}_0$. The nematic degrees of freedom being frozen, the governing equations reduce to the mass and force balances

$$\dot{\rho} + \mathrm{div}(\rho \mathbf{v}) = 0, \qquad \mathrm{div}\,\mathbf{T} - \rho\left(\dot{\mathbf{v}} + (\boldsymbol{\nabla}\mathbf{v})\mathbf{v}\right) = 0. \quad (1)$$

All fields involved – mass density ρ, translational velocity $\mathbf{v}$, and Cauchy stress $\mathbf{T}$ – are spatial, and dotted quantities are partial time derivatives.

2.1 Ericksen's transversely isotropic fluid

The constitutive assumption for the stress put forward by Ericksen[3] as early as in 1960, when stripped of the viscous terms and under isothermal conditions, reduces to[‡]

$$\mathbf{T} = -\left(\pi(\rho)\,\mathbf{I} + \alpha(\rho)\,\mathbf{n}_0 \otimes \mathbf{n}_0\right). \quad (2)$$

[†] In the experiments reported in Ref. 10 the temperature was stabilised to within $\pm 0.1\,^\circ$C or less. Lord and Labes[19] experimented at room temperature. What was actually measured by both groups was the angle between the propagation direction and the direction of the uniform magnetic field used to align the molecules. Lord and Labes[19] applied fields up to 12 kOe, observing no change in the attenuation beyond 1 kOe. Mullen, Lüthi and Stephen[10] reported no field dependence between 0.5 and 5 kOe. Also the nematoacoustic analysis by Virga[17] is based on the hypothesis of a uniform and immobile director field. Lifting this assumption, as done by De Matteis and Virga[20], does not seem to make much of a difference – at least within the second-gradient theory developed in Ref. 17.

[‡] The tensor product between vectors $\mathbf{a}, \mathbf{b}$ operates on any vector $\mathbf{u}$ as follows: $(\mathbf{a} \otimes \mathbf{b})\mathbf{u} = (\mathbf{b} \cdot \mathbf{u})\,\mathbf{a}$ for all $\mathbf{u}$ (i.e., $(\mathbf{a} \otimes \mathbf{b})_{ij} = a_i b_j$ in any orthonormal basis). The tensor product between double tensors is defined analogously, so that $(\mathbf{A} \otimes \mathbf{I})\mathbf{E} = (\mathbf{I} \cdot \mathbf{E})\mathbf{A} = (\mathrm{tr}\,\mathbf{E})\mathbf{A}$, $\mathbf{I}$ being the identity on vectors. The inner product between double tensors is defined as $\mathbf{M} \cdot \mathbf{L} = \mathrm{tr}(\mathbf{M}^\top \mathbf{L})$. The trace tr is the unique linear form on double tensors such that $\mathrm{tr}(\mathbf{a} \otimes \mathbf{b}) = \mathbf{a} \cdot \mathbf{b} = a_i b_i$ (sum over i). We use few fourth-order tensors, denoted by blackboard bold symbols.

Both the spherical and the *uniaxial* component are assumed to depend only on the mass density. It is worth rewriting (2) as the sum of a spherical and a *deviatoric* (i.e., traceless) component:

$$\mathbf{T} = -\left(\pi(\rho) + \tfrac{1}{3}\alpha(\rho)\right)\mathbf{I} - \alpha(\rho)\left(\mathbf{n}_0 \otimes \mathbf{n}_0 - \tfrac{1}{3}\mathbf{I}\right), \quad (3)$$

so as to make apparent that $\pi(\rho)$ is not the pressure, which depends also on the anisotropic coefficient $\alpha(\rho)$. Adopting (2) transforms the force balance $(1)_2$ into

$$\rho\left(\dot{\mathbf{v}} + (\boldsymbol{\nabla}\mathbf{v})\mathbf{v}\right) = -\boldsymbol{\nabla}\pi - (\mathbf{n}_0 \otimes \mathbf{n}_0)\boldsymbol{\nabla}\alpha. \quad (4)$$

Linear acoustic waves are obtained via a regular perturbation expansion of $(1)_1$ and (4) around the unperturbed state:

$$\rho_\varepsilon = \rho_0 + \varepsilon\rho_1 + o(\varepsilon), \qquad \mathbf{v}_\varepsilon = \varepsilon\mathbf{v}_1 + o(\varepsilon) \quad (5)$$

where ε is a smallness parameter. Assumptions (5) entail

$$\begin{aligned} \pi(\rho_\varepsilon) &= \pi(\rho_0) + \varepsilon\,\pi'(\rho_0)\rho_1 + o(\varepsilon), \\ \alpha(\rho_\varepsilon) &= \alpha(\rho_0) + \varepsilon\,\alpha'(\rho_0)\rho_1 + o(\varepsilon). \end{aligned} \quad (6)$$

Since $\boldsymbol{\nabla}\rho_0 = 0$, the $O(1)$ set of equations is trivially satisfied. The $O(\varepsilon)$ set is comprised of the acoustic equations

$$\dot{\rho}_1 + \rho_0\,\mathrm{div}\,\mathbf{v}_1 = 0, \qquad \rho_0\dot{\mathbf{v}}_1 = -\mathbf{A}_0\boldsymbol{\nabla}\rho_1, \quad (7)$$

where the acoustic tensor $\mathbf{A}_0$ is given by

$$\mathbf{A}_0 = \pi'(\rho_0)\mathbf{I} + \alpha'(\rho_0)\mathbf{n}_0 \otimes \mathbf{n}_0. \quad (8)$$

Equations (7) entail the anisotropic wave equation

$$\ddot{\rho}_1 - \mathrm{div}(\mathbf{A}_0\boldsymbol{\nabla}\rho_1) = 0. \quad (9)$$

A plane wave

$$\rho_1(\mathbf{r},t) = A\cos(\mathbf{k}\cdot\mathbf{r} - \omega t) \quad (10)$$

with A the wave amplitude, $\mathbf{k}$ the wave vector, its modulus $|\mathbf{k}|$ the wave number, and ω the angular frequency, solves (9) if its phase velocity $v_s := \omega/|\mathbf{k}|$ solves the quadratic equation

$$v_s^2 = \pi'(\rho_0) + \alpha'(\rho_0)(\mathbf{k}\cdot\mathbf{n}_0/|\mathbf{k}|)^2. \quad (11)$$

It is known from empirical evidence that $|\alpha'(\rho_0)| \ll \pi'(\rho_0)$, implying that to a very good approximation

$$v_s = \sqrt{\pi'(\rho_0)}\left(1 + \frac{\alpha'(\rho_0)}{2\,\pi'(\rho_0)}(\cos\theta)^2\right), \quad (12)$$

where θ is the angle between $\mathbf{k}$ and $\mathbf{n}_0$. As regards the angular dependence of the sound speed v_s, (12) matches perfectly with the experimental findings reported in Ref. 10 and the predictions provided by the competing second-gradient theory [17].

With this being said, there are several good reasons to reject the simplistic assumption (2). They were hinted at in the Introduction, and will be discussed in depth below. In particular, the bias implicit in (2) causes a conflict between anisotropy and hyperelasticity. In a later section of the very same paper [3] where the constitutive equations leading to (2) were proposed, after assuming a free-energy density depending only on mass density and temperature, Ericksen wrote that 'the form of the Clausius inequality most often used in irreversible thermodynamics ... will lead to some restrictions on the coefficients occurring in [the above constitutive equations]' – which he did not investigate there. In a paper he published soon after [22], the term corresponding to the uniaxial component in (2) was already dropped.

As a matter of fact, it turns out that the only way to let (2) satisfy such restrictions is to take α *null*, which entails a spherical acoustic tensor. This is proved in Appendix A in the general context of finite elasticity. A weaker result, i.e., that $\alpha'(\rho_0)$ should vanish is readily obtained by linearising (2) around ρ_0. On account of the fact that $\rho_1 = -\rho_0\,\mathrm{tr}\,\mathbf{E}$ (with $\mathbf{E}$ the infinitesimal strain), one finds that the elastic tensor $\mathbb{C}_0$ equals $\rho_0\mathbf{A}_0 \otimes \mathbf{I}$, with $\mathbf{A}_0$ the acoustic tensor in (8). Therefore, $\mathbb{C}_0$ has the major symmetry if and only if $\mathbf{A}_0$ is spherical, i.e., if and only if $\alpha'(\rho_0) = 0$.

2.2 A hyperelastic transversely isotropic material

We now proceed to build up the simplest strain-energy density fit to describe the anisotropic elastic response of a compressible liquid crystal in its nematic phase. To this aim we compare its current configuration (characterised by a uniform director field) with a reference configuration in its *isotropic* phase. Consider a small LC sample whose reference shape is a spherical ball B_ε of radius ε. Our strain-energy choice stems from the assumption, illustrated in Fig. 1, that in the nematic phase the relaxed shape of the formerly spherical ball becomes an ellipsoid of revolution sharing the same volume. Therefore, in order to represent the intrinsic anisotropy associated with the nematic phase we introduce the *asphericity factor* $a(\rho)$ such that the area of the cross section normal to the symmetry axis equals $\pi\varepsilon^2/(1+a(\rho))$. As a consequence, a prolate (oblate) ellipsoid is obtained whenever $a(\rho)$ is positive (negative). This factor assumes therefore the role of an order parameter describing the loss of spherical symmetry of the *centre-centre* pair correlation function of LC molecules due to the isotropic-to-nematic phase transition [23–26]. Since the positional components of the correlation function vary smoothly across the transition [27], the asphericity factor is expected to be small. Nonetheless, it may affect significantly the elastic properties of the nematic phase.

The above argument motivates the introduction of the following stored energy density (with respect to mass):

$$\sigma(\mathbf{F},\mathbf{n}_0) = \hat{\sigma}(\rho,\mathbf{n}_0,\mathring{\mathbf{B}}) :=$$
$$\sigma_{\texttt{iso}}(\rho) + \tfrac{1}{2}\mu(\rho)\,\text{tr}\big(\boldsymbol{\Psi}(\rho,\mathbf{n}_0)^{-1}\mathring{\mathbf{B}} - \mathbf{I}\big), \quad (13)$$

where $\mathbf{F}$ is the deformation gradient, ρ is related to it through mass conservation: $\rho = \rho_0/J$, with $J := \det\mathbf{F}$, $\mathring{\mathbf{B}} := \mathring{\mathbf{F}}\mathring{\mathbf{F}}^\top$ is the left Cauchy-Green strain tensor associated with the isochoric component of the deformation gradient $\mathring{\mathbf{F}} := J^{-1/3}\mathbf{F}$, and

$$\boldsymbol{\Psi}(\rho,\mathbf{n}) := \big(1 + a(\rho)\big)^2\,\mathbf{n}\otimes\mathbf{n} + \big(1 + a(\rho)\big)^{-1}\big(\mathbf{I} - \mathbf{n}\otimes\mathbf{n}\big) \quad (14)$$

is a *shape tensor*, embodying information on the symmetry-breaking nematic direction and the asphericity factor associated with the transformation illustrated in Fig. 1.

(a)   (b)
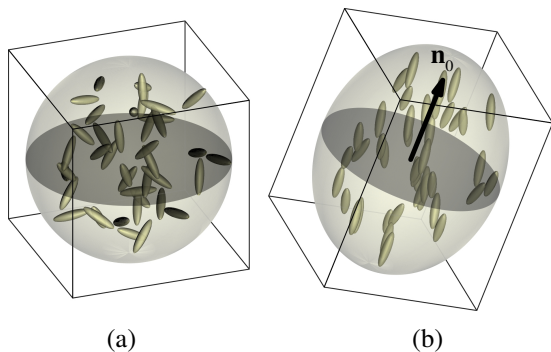
Fig. 1 Molecular cartoon illustrating two isovolumic shear-stress free configurations of a small blob of liquid crystal, respectively in the isotropic (a) and in the nematic phase (b). Bounding boxes help visualising the action of the isochoric deformation gradient $\mathbf{F}$ from (a) to (b). Cube (a) is the image under the *inverse* deformation gradient $\mathbf{F}^{-1}$ of parallelepiped (b), whose long axis is aligned with the nematic director $\mathbf{n}_0$.

The first term on the right side of (13) accounts for the effects of non-volume-preserving deformations. It is the dominant term in the strain-energy density – indeed, the only one for standard elastic fluids. The second term is the simplest frame-indifferent, positive-definite, symmetry-allowed function of the pair $(\mathring{\mathbf{F}},\mathbf{n}_0)$ vanishing if (and only if) $\mathring{\mathbf{B}} = \boldsymbol{\Psi}(\rho,\mathbf{n}_0)$. Its dependence on the *left* strain tensor $\mathring{\mathbf{B}}$, rather than on the *right* strain $\mathring{\mathbf{C}} := \mathring{\mathbf{F}}^\top\mathring{\mathbf{F}}$, reflects the essential fact that the director field $\mathbf{n}$ is a *spatial* field independent of (though dynamically coupled to) the translational motion. This term is formally analogous to the representation given by DeSimone and Teresi[28] of the trace formula originally proposed by Warner, Terentjev and co-workers[29–31] to model the soft elastic response of nematic elastomers. What is specific to the present theory is the crucial dependence of the shape tensor on the density via the asphericity factor, as established by (14). We

allow also the (strictly positive) modulus $\mu(\rho)$ to be density-dependent, but this is inessential.

As we prove in Appendix B, the hyperelastic theory stemming from (13)–(14) provides the simplest extension to finite elasticity of the small-displacement theory intimated by Mullen et al.[10] to make sense of their experimental results.

Assumptions (13)–(14) entail the following prescription for the Cauchy stress (cf. Appendix B):

$$\mathbf{T}(\rho,\mathbf{n}_0,\mathring{\mathbf{B}}) = -\hat{p}(\rho,\mathbf{n}_0,\mathring{\mathbf{B}})\,\mathbf{I}$$
$$+ \rho\,\mu(\rho)\,\text{dev}\big(\boldsymbol{\Psi}(\rho,\mathbf{n}_0)^{-1}\mathring{\mathbf{B}}\big), \quad (15)$$

where the product $\rho\mu(\rho)$ appears to be a shear modulus, dev is the deviatoric projector: $\text{dev}\,\mathbf{L} = \mathbf{L} - \tfrac{1}{3}(\text{tr}\,\mathbf{L})\mathbf{I}$, and

$$\hat{p}(\rho,\mathbf{n}_0,\mathring{\mathbf{B}}) := \rho^2\times$$
$$\Big(\sigma_{\texttt{iso}}'(\rho) + \tfrac{1}{2}\mu'(\rho)\,\text{tr}\big(\boldsymbol{\Psi}(\rho,\mathbf{n}_0)^{-1}\mathring{\mathbf{B}} - \mathbf{I}\big) \quad (16)$$
$$- \frac{3a'(\rho)}{2\big(1+a(\rho)\big)}\mu(\rho)\big(\text{dev}(\mathbf{n}_0\otimes\mathbf{n}_0)\big)\cdot\big(\boldsymbol{\Psi}(\rho,\mathbf{n}_0)^{-1}\mathring{\mathbf{B}}\big)\Big).$$

Consistently with the result stated in Sec. 2.1, (2) and (15) do not match. In a sense, however, (15) does not depart too much from (2) in the regime of interest, as we shall see below.

The unperturbed state of the NLC is characterised by a density equal to ρ_0 and a spherical stress tensor $\mathbf{T}_0$:

$$\text{dev}\,\mathbf{T}_0 = 0. \quad (17)$$

Equations (15) and (17) imply that the equilibrium strain $\mathring{\mathbf{B}}_0$ equals the shape tensor:

$$\mathring{\mathbf{B}}_0 = \boldsymbol{\Psi}(\rho_0,\mathbf{n}_0). \quad (18)$$

Then, (16) yields the equilibrium pressure

$$p_0 := \hat{p}(\rho_0,\mathbf{n}_0,\mathring{\mathbf{B}}_0) = \rho_0^2\sigma_{\texttt{iso}}'(\rho_0) \quad (19)$$

and (15) the equilibrium stress

$$\mathbf{T}_0 := \mathbf{T}(\rho_0,\mathbf{n}_0,\mathring{\mathbf{B}}_0) = -p_0\mathbf{I}. \quad (20)$$

Coherently, the reference configuration ($\mathring{\mathbf{B}} = \mathbf{I}$) is not shear-stress free in the nematic phase, unless $a_0 := a(\rho_0) = 0$:

$$\mathbf{T}(\rho_0,\mathbf{n}_0,\mathbf{I}) = -\hat{p}(\rho_0,\mathbf{n}_0,\mathbf{I})\,\mathbf{I}$$
$$- \frac{3+3a_0+a_0^2}{(1+a_0)^2}a_0\rho_0\mu_0\,\text{dev}\big(\mathbf{n}_0\otimes\mathbf{n}_0\big) \quad (21)$$

with

$$\hat{p}(\rho_0,\mathbf{n}_0,\mathbf{I}) = p_0 + \frac{3+3a_0+a_0^2}{(1+a_0)^3}a_0\rho_0^2 a'(\rho_0)\mu_0$$
$$+ \frac{3+2a_0}{2(1+a_0)^2}a_0^2\rho_0^2\mu'(\rho_0). \quad (22)$$

2.3 A slightly compressible anisotropic fluid

The theory we put forward in the preceding section is fairly general. Formally, it applies to any trasversely isotropic material, for finite deformations of any amplitude. The application we have in mind is, on the contrary, quite specific: the linear acoustic – i.e., *quasi*-equilibrium – response of a *quasi*-incompressible and slightly anisotropic NLCs, which – as all liquids – are hard to compress: tiny density variations should imply fairly large pressure changes. In addition, their faint anisotropic compressibility, however small, should be quite sensitive to small changes in density, in order to account for the angular dependence of the sound speed (cf. (12)).

The perturbative setting fit to represent the asymptotic regime of interest will now be identified, by introducing the *scaled density variation*

$$\xi := \rho/\rho_0 - 1 \tag{23}$$

and the *isotropic pressure function*

$$\rho \mapsto p_{\texttt{iso}}(\rho) = \rho^2 \sigma'_{\texttt{iso}}(\rho), \tag{24}$$

and positing

$$p_{\texttt{iso}}\big(\rho_0(1+\xi)\big) = p_0 + \rho_0 p_1 \xi + o(\xi). \tag{25}$$

Quasi-incompressibility implies the (positive) bulk modulus $\rho_0 p_1$ to be much larger than the (positive) unperturbed pressure p_0. This, in turn, is much larger than the pressure perturbation envisaged in the linear acoustic regime:

$$\rho_0 p_1 \gg p_0 \gg \rho_0 p_1 |\xi|. \tag{26}$$

Next, we formalise the hypothesis that the asphericity factor $a(\rho)$ is *uniformly* small near ρ_0 by positing

$$a\big(\rho_0(1+\xi)\big) = a_0 + a_1 \xi + o(\xi) \tag{27}$$

and assuming

$$|a_0| \ll 1. \tag{28}$$

In contrast to a_0, the *sensitivity coefficient* $a_1 = \rho_0 a'(\rho_0)$ is *not* required to be small, since assumption (26) ensures that $|\xi| \ll 1$. This fact will play a key role in our further considerations. Henceforth, the shape tensor (14) will be treated as a small perturbation of the identity. In this approximation, (18), (21) and (22) simplify respectively to

$$\mathring{\mathbf{B}}_0 = \mathbf{I} + 3 a_0 \mathrm{dev}\big(\mathbf{n}_0 \otimes \mathbf{n}_0\big) + o(a_0), \tag{29a}$$

$$\mathbf{T}(\rho_0, \mathbf{n}_0, \mathbf{I}) = -\hat{p}(\rho_0, \mathbf{n}_0, \mathbf{I})\,\mathbf{I}$$
$$- 3 a_0 \rho_0 \mu_0 \mathrm{dev}\big(\mathbf{n}_0 \otimes \mathbf{n}_0\big) + o(a_0), \tag{29b}$$

$$\hat{p}(\rho_0, \mathbf{n}_0, \mathbf{I}) = p_0 + 3 a_1 a_0 \rho_0 \mu_0 + o(a_0). \tag{29c}$$

Finally, we implement the hypothesis that the stored energy density (13) is dominated by its first term by positing

$$\mu\big(\rho_0(1+\xi)\big) = \mu_0 + \mu_1 \xi + o(\xi) \tag{30}$$

and assuming the *shear modulus* $\rho_0 \mu_0$ to be much smaller than the *bulk modulus* $\rho_0 p_1$:

$$\mu_0 = \eta p_1, \quad \text{with} \quad \eta \ll 1. \tag{31}$$

2.4 Angular dependence of the sound speed

We now look for travelling plane waves of the form

$$\mathbf{u}_\varepsilon(\mathbf{r},t) = \varepsilon\,\mathbf{u}(\mathbf{r},t) = \varepsilon\,\mathrm{Re}\big(\mathbf{w}(\mathbf{r},t)\big), \tag{32a}$$

$$\mathbf{w}(\mathbf{r},t) = \exp\big(i(\mathbf{k}\cdot\mathbf{r} - \omega t)\big)\mathbf{a}, \tag{32b}$$

where $\mathbf{u}_\varepsilon$ is a small-amplitude displacement field, characterised by the non-dimensional smallness parameter ε, the vector amplitude $\mathbf{a}$, the wave vector $\mathbf{k} = k\mathbf{e}$ (with $|\mathbf{e}| = 1$ and wave number $k > 0$), and the angular frequency ω. All of the above quantities are real. The complex exponential form in (32b) will turn out especially useful in Sec. 3.2, where the wave vector itself will be complexified, in order to represent possibly attenuated waves.

To avoid inessential complications, we will neglect terms of order $O(a_0)$ and $o(\varepsilon)$. Within these approximations, ansatz (32) implies

$$\dot{\mathbf{v}} = -\varepsilon\,\rho_0 \omega^2 \mathrm{Re}(\mathbf{w}), \tag{33a}$$

$$\mathbf{F} = \mathbf{I} - \varepsilon\,\mathrm{Im}(\mathbf{w}\otimes\mathbf{k}), \tag{33b}$$

$$\xi = \varepsilon\,\mathrm{Im}(\mathbf{w}\cdot\mathbf{k}), \tag{33c}$$

$$\mathring{\mathbf{B}} = \mathbf{I} - \varepsilon\,\mathrm{Im}\big(\mathrm{dev}(\mathbf{w}\otimes\mathbf{k} + \mathbf{k}\otimes\mathbf{w})\big), \tag{33d}$$

$$\boldsymbol{\Psi} = \mathbf{I} + 3\varepsilon\,a_1 \mathrm{Im}(\mathbf{w}\cdot\mathbf{k})\,\mathrm{dev}(\mathbf{n}_0 \otimes \mathbf{n}_0). \tag{33e}$$

Equation (33c) establishes that the scaled density variation is $O(\varepsilon)$, as expected. Substituting (33c), (33d) and (33e) into (15), one computes $\mathbf{T} = \mathbf{T}_0 + \varepsilon\,\mathbf{T}_1 + o(\varepsilon)$, where

$$\mathbf{T}_1 = -\rho_0 p_1 \mathrm{Im}(\mathbf{w}\cdot\mathbf{k})\,\mathbf{I}$$
$$- \rho_0 \mu_0 \mathrm{Im}\big\{3 a_1^2(\mathbf{w}\cdot\mathbf{k})\mathbf{I} + \mathrm{dev}(\mathbf{w}\otimes\mathbf{k} + \mathbf{k}\otimes\mathbf{w}) \tag{34}$$
$$+ 3 a_1\big((\mathrm{dev}(\mathbf{w}\otimes\mathbf{k}))\cdot(\mathbf{n}_0\otimes\mathbf{n}_0)\mathbf{I} + (\mathbf{w}\cdot\mathbf{k})\mathrm{dev}(\mathbf{n}_0\otimes\mathbf{n}_0)\big)\big\},$$

whose divergence reads

$$\mathrm{div}\,\mathbf{T}_1 = -\rho_0 \mathrm{Re}\big(p_1(\mathbf{k}\otimes\mathbf{k})\mathbf{w} + \mu_0 \mathbf{M}\mathbf{w}\big), \tag{35}$$

where all anisotropic information is encoded in the symmetric tensor

$$\mathbf{M} := (\mathbf{k}\cdot\mathbf{k})\mathbf{I} + (1/3 + 3 a_1^2)(\mathbf{k}\otimes\mathbf{k})$$
$$+ 3 a_1\big((\mathbf{n}_0\cdot\mathbf{k})(\mathbf{k}\otimes\mathbf{n}_0 + \mathbf{n}_0\otimes\mathbf{k}) - \tfrac{2}{3}\mathbf{k}\otimes\mathbf{k}\big). \tag{36}$$

Substituting (33a) and (35) into (1)$_2$ leads to the eigenvalue problem

$$\left(p_1(\mathbf{k}\otimes\mathbf{k})+\mu_0\mathbf{M}\right)\mathbf{a}=\omega^2\mathbf{a}. \tag{37}$$

Expanding the wavelength $\lambda = 2\pi/k$ and the wave amplitude vector $\mathbf{a}$ in terms of the small parameter η (cf. (31)) gives

$$\lambda_\eta = \lambda_0 + \eta\,\lambda_1 + o(\eta), \tag{38a}$$
$$\mathbf{a}_\eta = \mathbf{a}_0 + \eta\,\mathbf{a}_1 + o(\eta). \tag{38b}$$

The $O(1)$ solution to (37) yields a longitudinal wave vector $\mathbf{a}_0$ and an isotropic sound speed v_0, as expected:

$$\mathbf{a}_0 = A_0\mathbf{e} \ \text{ with } A_0 > 0, \qquad v_0 = \frac{\omega}{2\pi}\lambda_0 = \sqrt{p_1}. \tag{39}$$

The $O(\eta)$ problem reads

$$-2(\lambda_1/\lambda_0)A_0\mathbf{e} + (\lambda_0/2\pi)^2 A_0\mathbf{M}_0\mathbf{e} = (\mathbf{I}-\mathbf{e}\otimes\mathbf{e})\mathbf{a}_1, \tag{40}$$

with

$$(\lambda_0/2\pi)^2\,\mathbf{M}_0\mathbf{e} = \left(4/3 - 2a_1 + 3a_1^2 + 3a_1(\cos\theta)^2\right)\mathbf{e}$$
$$+ 3a_1(\cos\theta)\mathbf{n}_0, \tag{41}$$

where θ is the angle between $\mathbf{e}$ and $\mathbf{n}_0$. The solubility condition of (40) yields the $O(\eta)$ anisotropic correction to the speed of sound:

$$v_s/v_0 = 1 + \eta\left(2/3 - a_1 + 3a_1^2/2 + 3a_1(\cos\theta)^2\right). \tag{42}$$

Then, solving (40) (in the subspace orthogonal to $\mathbf{e}$) delivers the $O(\eta)$ correction to the wave amplitude vector:

$$\mathbf{e}\times\mathbf{a}_1 = 3a_1A_0(\cos\theta)\mathbf{e}\times\mathbf{n}_0. \tag{43}$$

Solution (43) exhibits the existence of an $O(\eta)$ transversely polarised component in the plane spanned by $\mathbf{n}_0$ and $\mathbf{e}$, whose amplitude is maximal when $\theta = \pi/4$:

$$\mathbf{a}_1 = \tfrac{3}{2}a_1A_0(\sin 2\theta)\mathbf{t}, \tag{44}$$

with $\mathbf{t}$ the unit vector orthogonal to $\mathbf{e}$ in $\text{span}\{\mathbf{n}_0,\mathbf{e}\}$ such that $\mathbf{t}\cdot\mathbf{n}_0 > 0$. The wave amplitude vector $\mathbf{a}$ is slightly tilted towards the nematic director if $a_1 > 0$, away from it if $a_1 < 0$. As far as the angular dependence of the sound speed is concerned, (42) is completely satisfactory. However, the underlying model is obviously unable to account for the important frequency dependence and the related attenuation systematically observed in experiments [10,19,32,33]. This issue will be attacked in Sec. 3.

A more accurate calculation would add insignificant terms of order $O(a_0)$ to the coefficient of η in (42), changing it into

$$2/3 - a_1 + 3a_1^2/2 + O(a_0) + (3 + O(a_0))a_1(\cos\theta)^2. \tag{45}$$

We conclude that, while the precise value of the asphericity factor is immaterial (as long as it is small), what really matters is the value of its derivative. In particular, the speed of sound is maximal or minimal when the direction of propagation is along the nematic director, depending on whether the asphericity factor increases or decreases with increasing density. The experimental evidence reported in Refs. 10, 19 points to a positive value of a_1.

3 Nematic relaxation

The hyperelastic theory set up in Sec. 2.2 misses the effects of molecular rearrangements which, while not affecting the macroscopic deformation of the NLC, do make the ensuing shear stress relax to zero whenever its macroscopic evolution is sufficiently slow. Roughly speaking, these microscopic rearrangements drive the liquid to lower energy states. A convenient caricature of their macroscopic effects is obtained by postulating that the relaxed configuration evolves on a characteristic time scale, steering towards a moving target, the actual configuration. This establishes a competition between the relaxation and the loading dynamics, which is at the origin of the frequency dependence of effective elastic moduli. Interestingly, a similar idea is already outlined in the last section of the seventh volume of the Course of Theoretical Physics by Landau and Lifshitz [34].
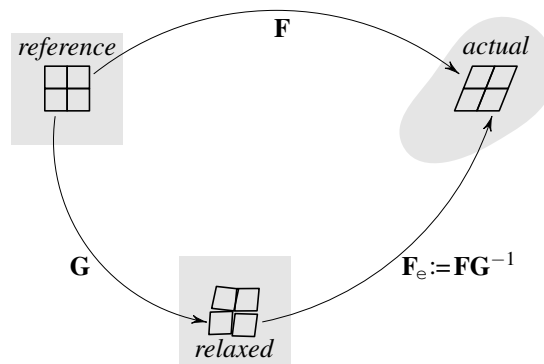
Fig. 2 Instantaneous decomposition of the deformation gradient $\mathbf{F}$ into a relaxing and an effective component. Disarrangements in the lower cartoon are meant to illustrate the fact that, contrary to $\mathbf{F}$, the relaxing tensor field $\mathbf{G}$ and the effective deformation field $\mathbf{F}_e$ need not be gradients.

We are thus motivated to split the deformation gradient $\mathbf{F}$ into the product of a *relaxing deformation* $\mathbf{G}$ and an *effective deformation* $\mathbf{F}_e$ (cf. Fig. 2):

$$\mathbf{F} = \mathbf{F}_e\mathbf{G}. \tag{46}$$

This decomposition is at the heart of a continuum theory such as ours, which models the (typically inelastic) dynamics of

materials undergoing both macroscopic deformation and microscopic relaxation with no resort to memory functionals. It formalises the idea that their response results from two distinct, intertwined processes. At each time, the current relaxing deformation maps the (conventional) reference configuration to the current relaxed configuration, while the effective deformation gauges the difference between the actual configuration and the current relaxed state. Therefore, it is sensible to assume that the stored energy density depends on $\mathbf{F}$ only through $\mathbf{F}_e$ (hence its label *effective*).

The relaxing deformation $\mathbf{G}$ is a time-dependent tensor field, taking values in the proper special linear group SL^+ (the Lie group of double tensors whose determinant equals $+1$). This modelling choice is prompted by the fact that no molecular reshuffling can accommodate the effects of a volume change and, as a consequence, only the deviatoric component of the stress may relax to zero. Since the relaxed configuration is defined only elementwise[11], in (46) the only gradient is $\mathbf{F}$: the tensor field $\mathbf{G}$ need *not* be a gradient, and the effective deformation $\mathbf{F}_e$ has to compensate its integrability defect (cf. Fig. 2).

After introducing the *inverse relaxing strain*

$$\mathbf{H} := \left(\mathbf{G}^\top \mathbf{G}\right)^{-1} \tag{47}$$

and the isochoric effective left Cauchy-Green strain

$$\mathring{\mathbf{B}}_e := \mathring{\mathbf{F}}_e \mathring{\mathbf{F}}_e^\top = \mathring{\mathbf{F}} \mathbf{H} \mathring{\mathbf{F}}^\top, \tag{48}$$

we just substitute $\mathring{\mathbf{B}}$ with $\mathring{\mathbf{B}}_e$ in (13), obtaining the stored energy density

$$\widetilde{\sigma}(\mathbf{F}, \mathbf{n}_0; \mathbf{H}) := \hat{\sigma}(\rho, \mathbf{n}_0, \mathring{\mathbf{B}}_e) = \\ \sigma_{\mathtt{iso}}(\rho) + \tfrac{1}{2}\mu(\rho)\operatorname{tr}\left(\mathbf{\Psi}(\rho, \mathbf{n}_0)^{-1}\mathring{\mathbf{B}}_e - \mathbf{I}\right), \tag{49}$$

where $\rho = \rho_0/J = \rho_0/(\det \mathbf{F}_e)$. Since the relaxing deformation $\mathbf{G}$ enters (49) only through the corresponding strain $\mathbf{H}$, we are naturally led to introduce the manifold $\mathscr{R}$ of inverse relaxing strains as the intersection of the proper special linear group SL^+ and the space of symmetric double tensors Sym:

$$\mathscr{R} := \mathsf{SL}^+ \cap \mathsf{Sym}. \tag{50}$$

The Cauchy stress is still given by (15), provided that $\mathring{\mathbf{B}}$ is substituted by $\mathring{\mathbf{B}}_e$:

$$\mathbf{T}(\rho, \mathbf{n}_0, \mathring{\mathbf{B}}_e) = -\hat{p}(\rho, \mathbf{n}_0, \mathring{\mathbf{B}}_e)\mathbf{I} \\ + \rho\,\mu(\rho)\operatorname{dev}\left(\mathbf{\Psi}(\rho, \mathbf{n}_0)^{-1}\mathring{\mathbf{B}}_e\right). \tag{51}$$

Of course, balance equations (1), supplemented with the constitutive prescription (51), need to be complemented by an evolution equation along $\mathscr{R}$ governing the relaxational degrees of freedom.

3.1 Relaxation dynamics

Inspired by ideas presented by Rajagopal and Srinivasa[35] and by DiCarlo and co-workers[11,36,37], we hypothesise a viscous-like dynamics for the inverse relaxing strain, described by a steepest-descent equation on the relaxing strain manifold $\mathscr{R}$:

$$\gamma\dot{\mathbf{H}} = -\rho_0\mathbb{P}_{\mathbf{H}}\frac{\partial\widetilde{\sigma}}{\partial\mathbf{H}}. \tag{52}$$

The scalar coefficient $\gamma > 0$ is a viscosity modulus, and $\mathbb{P}_{\mathbf{H}}$ is the orthogonal projector from the space of double tensors onto the subspace $\mathsf{T}_{\mathbf{H}}\mathscr{R}$ tangent to $\mathscr{R}$ at $\mathbf{H}$:

$$\mathbb{P}_{\mathbf{H}} = \mathsf{sym} - \frac{\mathbf{H}^{-1}\otimes\mathbf{H}^{-1}}{\|\mathbf{H}^{-1}\|^2}, \tag{53}$$

with sym the orthogonal projector onto Sym. Equation (53) is an easy consequence of the formula for the derivative of the determinant

$$\det(\mathbf{H} + \varepsilon\,\mathbf{L}) = (\det\mathbf{H})(1 + \varepsilon\,\mathbf{H}^{-\top}\cdot\mathbf{L}) + o(\varepsilon) \tag{54}$$

($= 1 + \varepsilon\,\mathbf{H}^{-1}\cdot\mathbf{L} + o(\varepsilon)$, since $\mathbf{H} \in \mathscr{R}$), implying that the unit normal to $\mathsf{T}_{\mathbf{H}}\mathscr{R}$ is $\mathbf{H}^{-1}/\|\mathbf{H}^{-1}\|$.

The evolution equation (52) is consistent with the dissipation principle establishing that the power dissipated – defined as the difference between the power expended and the time derivative of the free energy – should be non-negative for all body-parts at all times. This condition localises into

$$\mathbf{S}\cdot\dot{\mathbf{F}} - \rho_0\dot{\widetilde{\sigma}} \geq 0, \tag{55}$$

with $\mathbf{S}$ the Piola stress. Since $\mathbf{S} = \rho_0(\partial\widetilde{\sigma}/\partial\mathbf{F})$ (cf. Appendix B), (55) reduces to

$$\rho_0\frac{\partial\widetilde{\sigma}}{\partial\mathbf{H}}\cdot\dot{\mathbf{H}} \leq 0. \tag{56}$$

Hypothesis (52) – sometimes justified by the heuristic criterion of maximum rate of dissipation[35] – satisfies requirement (56) in the simplest possible way.

On account of (49) and (48), we obtain explicitly

$$\frac{\partial\widetilde{\sigma}}{\partial\mathbf{H}} = \tfrac{1}{2}\mu(\rho)\mathring{\mathbf{F}}^\top\mathbf{\Psi}(\rho)^{-1}\mathring{\mathbf{F}} \in \mathsf{Sym} \tag{57}$$

which, substituted into (52), yields

$$\frac{2\gamma}{\rho_0\mu(\rho)}\dot{\mathbf{H}} - \frac{\mathbf{\Psi}(\rho)^{-1}\cdot\left(\mathring{\mathbf{B}}\mathring{\mathbf{B}}_e^{-1}\mathring{\mathbf{B}}\right)}{\|\mathbf{H}^{-1}\|^2}\mathbf{H}^{-1} \\ = -\mathring{\mathbf{F}}^\top\mathbf{\Psi}(\rho)^{-1}\mathring{\mathbf{F}}. \tag{58}$$

3.2 Frequency-dependent anisotropic sound speed

We return to the problem studied in Sec. 2.4, looking now for *attenuated* plane waves. We keep (32a) as is, but we change (32b) into

$$\mathbf{w}(\mathbf{r},t) = \exp\big(i(\hat{\mathbf{k}}\cdot\mathbf{r} - \omega t)\big)\mathbf{a}, \tag{59}$$

where

$$\hat{\mathbf{k}} := \mathbf{k} + i\mathbf{l} \quad (\mathbf{k},\mathbf{l}\ \text{real}) \tag{60}$$

is a *complex* wave vector, whose real part $\mathbf{k}$ parametrises the propagation direction and the wavelength, exactly as in Sec. 2.4, while its imaginary part $\mathbf{l}$ determines how fast the longitudinal and transverse components of the wave get damped. This viscous effect is the upshot of the relaxation dynamics introduced in Sec. 3.1.

As in Sec. 2.4, we shall neglect terms of order $O(a_0)$ and $o(\varepsilon)$. The deformation gradient $\mathbf{F}$, the scaled density variation ξ and the shape tensor $\mathbf{\Psi}$ are still represented by (33b), (33c) and (33e), respectively, provided that $\mathbf{k}$ is substituted by $\hat{\mathbf{k}}$ and (32b) by (59).

At equilibrium, the inverse relaxing strain $\mathbf{H}$ equals the identity $\mathbf{I}$. After positing

$$\mathbf{H} = \mathbf{I} + \varepsilon\,\mathbf{H}_1 \quad \text{with } \mathbf{H}_1 \in \mathrm{T}_{\mathbf{I}}\mathscr{R} \tag{61}$$

(i.e., symmetric and traceless), we linearise (58) accordingly. We obtain

$$\tau\,\dot{\mathbf{H}}_1 + \mathbf{H}_1 = \mathrm{Im}(\mathbf{K} + 3a_1\mathbf{N}), \tag{62}$$

after introducing the *relaxation time*

$$\tau := \frac{2\gamma}{\rho_0\mu_0} \tag{63}$$

and positing

$$\mathbf{K} := \mathrm{dev}(\mathbf{w}\otimes\hat{\mathbf{k}} + \hat{\mathbf{k}}\otimes\mathbf{w}), \tag{64a}$$

$$\mathbf{N} := (\mathbf{w}\cdot\hat{\mathbf{k}})\,\mathrm{dev}(\mathbf{n}_0\otimes\mathbf{n}_0). \tag{64b}$$

Modulo an exponentially decaying transient, (62) is solved by

$$\mathbf{H}_1 = \mathrm{Im}\big((1 - i\omega\tau)^{-1}(\mathbf{K} + 3a_1\mathbf{N})\big). \tag{65}$$

Consequently, from (61), (48) and (51) we get the effective isochoric strain

$$\begin{aligned}
\mathring{\mathbf{B}}_{\mathrm{e}} &= \mathbf{I} + \varepsilon\big(\mathbf{H}_1 - \mathrm{Im}(\mathbf{K})\big) \\
&= \mathbf{I} + \varepsilon\,\mathrm{Im}\big((1 - i\omega\tau)^{-1}(i\omega\tau\mathbf{K} + 3a_1\mathbf{N})\big)
\end{aligned} \tag{66}$$

and the $O(\varepsilon)$ increment of the Cauchy stress

$$\begin{aligned}
\mathbf{T}_1 = &-\rho_0 p_1 \mathrm{Im}(\mathbf{w}\cdot\hat{\mathbf{k}})\,\mathbf{I} \\
&+ \rho_0\mu_0 \mathrm{Im}\big\{ i\omega\tau(1 - i\omega\tau)^{-1}\big(3a_1^2(\mathbf{w}\cdot\hat{\mathbf{k}})\mathbf{I} + \mathbf{K} \\
&+ 3a_1\big((\mathrm{dev}(\mathbf{w}\otimes\hat{\mathbf{k}}))\cdot(\mathbf{n}_0\otimes\mathbf{n}_0)\,\mathbf{I} + \mathbf{N}\big)\big)\big\},
\end{aligned} \tag{67}$$

whose divergence reads

$$\mathrm{div}\,\mathbf{T}_1 = -\rho_0 \mathrm{Re}\left(p_1(\hat{\mathbf{k}}\otimes\hat{\mathbf{k}})\mathbf{w} - \frac{i\omega\tau}{1 - i\omega\tau}\mu_0\mathbf{M}\mathbf{w}\right), \tag{68}$$

where the symmetric tensor $\mathbf{M}$ is still defined as in (36), provided that $\mathbf{k}$ is substituted by $\hat{\mathbf{k}}$. In the asymptotic limit $\omega\tau \to \infty$, the solid-like elastic response analysed in Sec. 2.4 is recovered: $\mathbf{H}_1$ tends to zero, and (66), (67) and (68) tend to (33d), (34) and (35), respectively.

In complete analogy with the procedure in Sec. 2.4, we substitute (33a) and (68) into $(1)_2$ and obtain the complex eigenvalue problem

$$\left(\hat{\mathbf{k}}\otimes\hat{\mathbf{k}} - \frac{i\omega\tau}{1 - i\omega\tau}\,\eta\,\mathbf{M}\right)\mathbf{a} = \frac{\omega^2}{p_1}\,\mathbf{a}, \tag{69}$$

where η is the small non-dimensional parameter introduced in (31). After supplementing expansions (38) with

$$\mathbf{l}_\eta = \mathbf{l}_0 + \eta\,\mathbf{l}_1 + o(\eta), \tag{70}$$

we perform a perturbation analysis of (69), split into its real and imaginary parts. At order $O(1)$, we obtain $\mathbf{l}_0 = 0$ and recover the same wave vector and isotropic sound speed given in (39). The real $O(\eta)$ problem reads

$$\begin{aligned}
2\frac{\lambda_1}{\lambda_0}A_0\mathbf{e} - &\left(\frac{\lambda_0}{2\pi}\right)^2 A_0\mathrm{Re}\left(\frac{i\omega\tau}{1 - i\omega\tau}\right)\mathbf{M}_0\mathbf{e} \\
&= (\mathbf{I} - \mathbf{e}\otimes\mathbf{e})\,\mathbf{a}_1,
\end{aligned} \tag{71}$$

with $\mathbf{M}_0\mathbf{e}$ given by (41). The solubility condition of (71) yields the $O(\eta)$ frequency-dependent, anisotropic correction to the speed of sound:

$$\frac{v_{\mathrm{s}}}{v_0} = 1 + \eta\,f(\omega\tau)\left(\tfrac{2}{3} - a_1 + \tfrac{3}{2}a_1^2 + 3a_1(\cos\theta)^2\right), \tag{72}$$

with

$$f(x) := \frac{x^2}{1 + x^2} \quad (x \geq 0). \tag{73}$$

The modulating function f behaves like $x \mapsto x^2$ for $x \to 0$ and like $x \mapsto 1 - (1/x)^2$ for $x \to \infty$. More interestingly, it is well approximated by the *linear* function $x \mapsto x/2$ in a rather large neighbourhood of $x = 1$ (cf. Fig. 3). As we shall discuss in depth in Sec. 4, this appears to be the regime relevant to the experiments motivating our modelling effort[10,19]. The same modulation affects also the $O(\eta)$ correction to the wave amplitude vector:

$$\mathbf{a}_1 = \tfrac{3}{2}a_1 A_0 f(\omega\tau)(\sin 2\theta)\mathbf{t}, \tag{74}$$

where $\mathbf{t}$ is the unit vector normal to $\mathbf{e}$ introduced in (44). Finally, solving the imaginary $O(\eta)$ problem

$$(\mathbf{I} + \mathbf{e}\otimes\mathbf{e})\mathbf{l}_1 = \frac{\lambda_0}{2\pi}\mathrm{Im}\left(\frac{i\omega\tau}{1 - i\omega\tau}\right)\mathbf{M}_0\mathbf{e}, \tag{75}$$
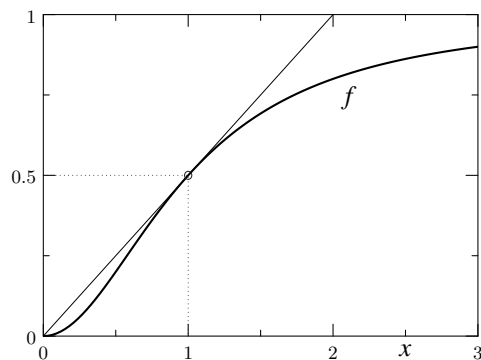
Fig. 3 Plot of the modulating function (73) in the range $[0,3]$. The affine approximation to f at $x=1$ is also plotted. Note that this is in fact linear, since its plot passes through the origin $(0,0)$.

delivers the attenuation vector

$$
\mathbf{l} = \eta \operatorname{Im}\left(\frac{i\omega\tau}{1-i\omega\tau}\right)\frac{\lambda_0}{2\pi}\left(\mathbf{I}-\tfrac{1}{2}\mathbf{e}\otimes\mathbf{e}\right)\mathbf{M}_0\mathbf{e}
$$

$$
= \eta\,\frac{\omega\tau}{1+(\omega\tau)^2}\frac{2\pi}{\lambda_0}\times \qquad (76)
$$

$$
\left(\left(\tfrac{2}{3}-a_1+\tfrac{3}{2}a_1^2+3a_1(\cos\theta)^2\right)\mathbf{e}+\tfrac{3}{2}a_1(\sin 2\theta)\mathbf{t}\right).
$$

It is noteworthy that the longitudinal and the transverse component of the attenuation vector depend on the angle θ exactly as the sound speed (cf. (72)) and the amplitude of the transverse wave (cf. (74)), respectively. Since Lord and Labes [19] give attenuation data in decibels per unit flight time rather than distance travelled, it is apposite to transform (76) accordingly, by multiplying the attenuation vector by the isotropic sound speed $(39)_2$:

$$
v_0\mathbf{l} = (\eta/\tau)f(\omega\tau)\times \qquad (77)
$$

$$
\left(\left(\tfrac{2}{3}-a_1+\tfrac{3}{2}a_1^2+3a_1(\cos\theta)^2\right)\mathbf{e}+\tfrac{3}{2}a_1(\sin 2\theta)\mathbf{t}\right),
$$

with f the modulating function (73). These and the previous results will be interpreted and compared with the cited experimental data in Sec. 4.

4 Discussion

After offering scattered comments on the qualitative agreement of our results with the experimental evidence published in the early seventies [10,19,32,33], we now proceed to a quantitative comparison between the predictions of our theory with the data by Lord and Labes [19] and Mullen et al. [10]. Both groups experimented on the same LC molecule, namely, N-(4-methoxybenzylidene)-4-butylaniline (MBBA)[§]. Since their

---

[§] Lieberman et al. [32] and Kemp and Letcher [33] worked with LC molecules different from MBBA: both groups with para-azoxyanisole (PAA), the second

data have been used also by De Matteis and Virga [20] to estimate the phenomenological parameters of their second-gradient theory, this will facilitate the comparison between our theory and theirs.

Our retrodictions, encapsulated in (72) and (77), depend on a handful of parameters: the unperturbed mass density ρ_0, the bulk modulus $\rho_0 p_1$, the shear modulus $\rho_0 \mu_0$, the anisotropic sensitivity coefficient a_1, and the relaxation time τ. The mass density is a standard material property: we take

$$
\rho_0 = 10^3\,\mathrm{kg/m^3}. \qquad (78)
$$

Lord and Labes [19] report that 'background attenuation varied from 2.18 dB/μs at 6 MHz to 0.37 dB/μs at 2 MHz.' After identifying their 'background attenuation' with the modulus of the attenuation (77) averaged over θ, this information translates into an equation independent of a_1 and η:

$$
\frac{f(12\cdot 10^6\,\pi\,\tau)}{f(4\cdot 10^6\,\pi\,\tau)} = \frac{2.18}{0.37} \qquad (79)
$$

(with f the modulating function (73) and τ in seconds), whose solution yields the relaxation time

$$
\tau = 2.11\cdot 10^{-8}\,\mathrm{s}. \qquad (80)
$$

Remarkably, this value coincides with the one ($2\cdot 10^{-8}$ s) estimated on different grounds by Mullen et al. [10]. Differently from them, we do not assume as a hypothesis that $\omega\tau\approx 1$, but find as a result that all of the experiments reported in Refs. 10, 19 fall in the interval

$$
0.265 \le \omega\tau \le 1.86. \qquad (81)
$$

We consider therefore our estimate (80) decidedly robust.

Next, to estimate the stiffness ratio η and the anisotropic sensitivity coefficient a_1, we combine the cited data on the background attenuation from Lord and Labes [19] with the data on the angular dependence of sound velocity provided by Mullen et al. [10], whose Fig. 2 shows that, at 21 °C and 10 MHz,

---

one also with p-azoxyphenetole (PAP). For this reason, their attenuation data – neither of them detected an anisotropic sound velocity – will not be used here. Moreover, the experimental findings of Kemp and Letcher [33] seem to indicate that, in the temperature and frequency range they explored (138–155 °C and 5–18 MHz for PAA, 116–129 °C and 3–15 MHz for PAP), the attenuation due to a 'hysteresis effect [of the] type [that] has been observed in very viscous liquids, glasses and metals' – as put by Lord and Labes [19] – was overshadowed by a qualitatively different dissipation mechanism. In fact, the attenuation data measured by Kemp and Letcher (in decibels per unit distance traveled) are in good agreement with the theory by Forster et al. [38], which dictates a quadratic dependence on frequency – in the same way as Leslie's theory does, when extended to compressible LCs [17,39]. At variance with that, the anisotropic attenuation measured by Lord and Labes in decibels per unit flight time depends linearly on frequency. The data reported by Lieberman et al. [32] are of no help in this respect, having being taken for only one frequency (1.83 MHz). This issue will be considered in a companion paper.

the experimentally measured difference between the speed of sound in the direction at an angle θ with respect to $\mathbf{n}_0$ and that in the direction normal to $\mathbf{n}_0$ is nicely interpolated by $1.25 \cdot 10^{-3} (\cos \theta)^2$ times the average sound speed. As for this last quantity, we may use the value $1.54 \cdot 10^3$ m/s measured by Mullen et al.[10] for 2 MHz at 22 °C, since scaling it to 10 MHz according to (72) affects it far beyond the third significant digit. The above pieces of information, plugged respectively into (77) and (72), provide the estimates[¶]

$$\eta = 1.99 \cdot 10^{-2}, \tag{82a}$$

$$a_1 = 3.27 \cdot 10^{-2}. \tag{82b}$$

Finally, using (72) and (39)$_2$ yields

$$p_1 = 2.37 \cdot 10^6 \, \text{m}^2/\text{s}^2, \tag{83}$$

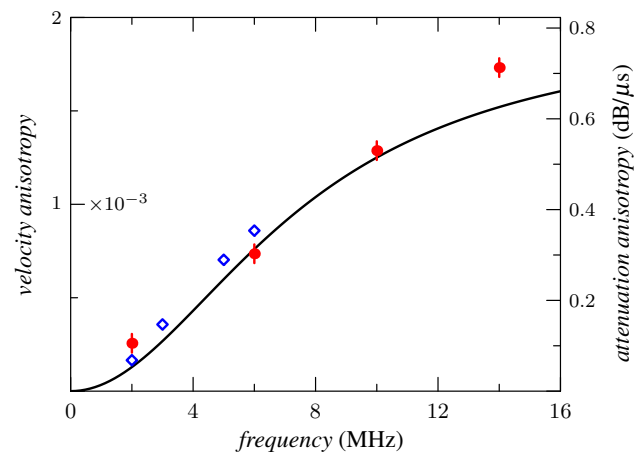which, combined with (78), (82a) and (31), delivers the following estimates for the bulk and shear moduli:

$$\rho_0 p_1 = 2.37 \, \text{GPa}, \tag{84a}$$

$$\rho_0 \mu_0 = 48.6 \, \text{MPa}. \tag{84b}$$

Note as a consistency check that all of the above estimates comply with the hypotheses introduced in Sec. 2.3.

A direct quantitative comparison between our results and experimental data from Refs. 10, 19 is provided in Fig. 4. Their less-than-perfect agreement is more than satisfactory, on account of the fact that our theoretical curve, far from being fitted to the eight experimental points in the figure, depends on only five parameters – two of which standard – identified on the basis of experimental information from the same sources[10,19], but *independent* of the data gathered in Fig. 4. Besides, a better agreement should not be expected since our model ignores all dissipation mechanisms different from the relaxation dynamics introduced in Sec. 3.1. In particular, it lacks the contribution of the Leslie-Ericksen viscous stress tensor, extended to compressible LCs[39] – which, contrariwise, is the only source of dissipation in the competing second-gradient theory[17,20]. This points to the need of extending the present model and to the interest of studying how the Leslie-Ericksen viscosities interact with the anisotropic compressibility peculiar to our theory. This would likely introduce at least one more relaxation time. But even in its present state, our model provides the first quantitatively based explanation of the structural relaxation process hypothesised long ago by Mullen et al.[10].

Also the constraint on the nematic director should be lifted, adding an Oseen-Frank term to the stored energy density, as

---

[¶] The simplistic assumption that the background attenuation is mimicked by suppressing the a_1 terms in (77) allows the stiffness ratio to be identified straightforwardly from this equation alone as $\eta = 2.05 \cdot 10^{-2}$. Then, the anisotropic sensitivity coefficient is obtained from (72) as $a_1 = 3.19 \cdot 10^{-2}$. Note that these estimates agree with those in (82) to two significant digits.

Fig. 4 Frequency dependence of the velocity anisotropy (left *y*-axis) and the attenuation anisotropy, defined as the difference between the attenuation along $\mathbf{n}_0$ and the attenuation in the direction normal to it (right *y*-axis). Circles with error bars represent experimental values of the velocity anisotropy taken from Fig. 3 of Ref. 10 (at a temperature of 27 °C). Diamonds reproduce the attenuation data from Fig. 2 of Ref. 19. The full line is the retrodiction of our theory for both velocity and attenuation anisotropy.

sketched in Appendix B. However, one of us has already proved[21] that director oscillations do not affect significantly the present results.

Finally, we point out that the present theory could be readily generalised to encompass temperature-dependent effects, including the critical behaviour close to the isotropic-to-nematic phase transition. To this end, one should first replace the nematic director with de Gennes' nematic order tensor $\mathbf{Q}$. This may be done simply by substituting the $\mathbf{n} \otimes \mathbf{n}$ terms in (14) with $\mathbf{Q} + \frac{1}{3}\mathbf{I}$, and adding the usual Landau-de Gennes thermodynamic potential to the free energy. Such a generalisation, however, should be handled with care, since the coefficients of the thermodynamic potential depend critically on density.

Acknowledgements

References

1 C. Oseen, *Trans. Faraday Soc.*, 1933, **29**, 883–900.

2 F. Frank, *Disc. Faraday Soc.*, 1958, **25**, 19–28.

---

3   J. L. Ericksen, *Arch. Rational Mech. Anal.*, 1960, **4**, 231–237.

4   F. Leslie, *Arch. Rat. Mech. Anal.*, 1968, **28**, 265283.

5   O. A. Kapustina, *Crystallogr. Rep.*, 2004, **49**, 680–692.

6   H.-Y. Kee, *Phys. Rev. E*, 2003, **67**, 073105.

7   J. S. Sandhu, H. Wang and W. J. Popek, *Proc. SPIE*, 2000, **3955**, 94–108.

8   J. S. Sandhu, R. A. Schmidt and P. J. La Rivière, *Med. Phys.*, 2009, **36**, 2324–2327.

9   Y. J. Kim and J. S. Patel, *Appl. Phys. Lett.*, 1999, **75**, 1985–1987.

10 M. E. Mullen, B. Lüthi and M. J. Stephen, *Phys. Rev. Lett.*, 1972, **28**, 799–801.

11 A. DiCarlo and S. Quiligotti, *Mech. Res. Commun.*, 2002, **29**, 449–456.

12 K. R. Rajagopal and A. R. Srinivasa, *Z. angew. Math. Phys.*, 2004, **55**, 861–893.

13 J. V. Selinger, M. S. Spector, V. A. Greanya, B. Weslowski, D. Shenoy and R. Shashidhar, *Phys. Rev. E*, 2002, **66**, 051708.

14 V. A. Greanya, M. S. Spector, J. V. Selinger, B. T. Weslowski and R. Shashidhar, *J. Appl. Phys.*, 2003, **94**, 7571–7575.

15 A. P. Malanoski, V. A. Greanya, B. T. Weslowski, M. S. Spector, J. V. Selinger and R. Shashidhar, *Phys. Rev. E*, 2004, **69**, 021705.

16 V. A. Greanya, A. P. Malanoski, B. T. Weslowski, M. S. Spector and J. V. Selinger, *Liq. Cryst.*, 2005, **32**, 933–941.

17 E. G. Virga, *Phys. Rev. E*, 2009, **80**, 031705.

18 D. J. Korteweg, *Arch. Néerl. Sci. Exactes Nat.*, 1901, **6**, 1–24.

19 A. E. Lord Jr. and M. M. Labes, *Phys. Rev. Lett.*, 1970, **25**, 570–572.

20 G. De Matteis and E. G. Virga, *Phys. Rev. E*, 2011, **83**, 011703.

21 S. S. Turzi, to appear (arXiv:1401.3979).

22 J. L. Ericksen, *Trans. Soc. Rheol.*, 1961, **5**, 23–34.

23 R. Berardi, A. P. J. Emerson and C. Zannoni, *J. Chem. Soc. Faraday Trans.*, 1993, **89**, 4069–4078.

24 L. Longa, G. Cholewiak, R. Trebin and G. Luckhurst, *Eur. Phys. J. E*, 2001, **4**, 51–57.

25 N. Phuong, G. Germano and F. Schmid, *J. Chem. Phys.*, 2001, **115**, 7227–7234.

26 G. Tiberio, L. Muccioli, R. Berardi and C. Zannoni, *Chem. Phys. Chem.*, 2009, **10**, 125–136.

27 M. Allen and M. Warren, *Phys. Rev. Lett.*, 1997, **78**, 1291–1294.

28 A. DeSimone and L. Teresi, *Eur. Phys. J. E*, 2009, **29**, 191–204.

29 E. M. Bladon, P. Terentjev and M. Warner, *J. Phys. II France*, 1994, **4**, 75–91.

30 M. Warner and E. M. Terentjev, *Prog. Polym. Sci.*, 1996, **21**, 853–891.

31 M. Warner and E. M. Terentjev, *Liquid Crystal Elastomers*, Oxford Science Publications, Oxford, 2003.

32 E. D. Lieberman, J. D. Lee and F. C. Moon, *Appl. Phys. Lett.*, 1971, **18**, 280–281.

33 K. A. Kemp and S. V. Letcher, *Phys. Rev. Lett.*, 1971, **27**, 1634–1636.

34 L. D. Landau and E. M. Lifshitz, in *Theory of Elasticity*, Pergamon Press, London, 1959, pp. 130–131.

35 K. R. Rajagopal and A. R. Srinivasa, *Int. J. Plast.*, 1998, **14**, 969–995.

36 A. DiCarlo, in *Surface and bulk growth unified*, ed. P. Steinmann and G. A. Maugin, Springer, 2005, pp. 56–64.

37 A. DeSimone, A. DiCarlo and L. Teresi, *Eur. Phys. J. E*, 2007, **24**, 303–310.

38 D. Forster, T. C. Lubensky, P. Martin, J. Swift and P. S. Pershan, *Phys. Rev. Lett.*, 1971, **26**, 1016–1019.

39 S. E. Monroe Jr., G. C. Wetsel Jr., M. R. Woodard and B. A. Lowry, *J. Chem. Phys.*, 1975, **63**, 5139–5144.

40 J. L. Ericksen, *Arch. Rational Mech. Anal.*, 1962, **10**, 189–196.

A   Ericksen's elastic fluid is hyperelastic only if isotropic

Ericksen's constitutive assumption (2) for the Cauchy stress translates into the following prescription for the Piola stress (cf. Appendix B):

$$\mathbf{S} = \varphi(J)\,\mathbf{F}^{-\top} + \psi(J)\,\mathbf{n}_0 \otimes \left(\mathbf{F}^{-1}\mathbf{n}_0\right), \tag{A.1}$$

where $J := \det\mathbf{F}\,(= \rho_0/\rho$ due to mass conservation) and

$$\varphi(J) := -J\pi(\rho_0/J), \quad \psi(J) := -J\alpha(\rho_0/J). \tag{A.2}$$

Since the power expended per unit reference volume is equal to $\mathbf{S}\cdot\dot{\mathbf{F}}$, prescription (A.1) is hyperelastic if and only if the derivative $\mathbb{D}(\mathbf{F}) := \partial\mathbf{S}/\partial\mathbf{F}$ has the major symmetry for all invertible $\mathbf{F}$:

$$\left(\mathbb{D}(\mathbf{F})\mathbf{L}\right)\cdot\mathbf{M} = \left(\mathbb{D}(\mathbf{F})\mathbf{M}\right)\cdot\mathbf{L} \tag{A.3}$$

for all double tensors $\mathbf{L},\mathbf{M}$. To prove that no anisotropic choice – i.e., $\alpha \neq 0 \Leftrightarrow \psi \neq 0$ – is hyperelastic, it suffices to check condition (A.3) on $\mathbf{F} = \lambda\,\mathbf{I}$ for all $\lambda > 0$, which greatly simplifies calculations. On spherical stretches (A.3) reduces to

$$\begin{aligned}\lambda^3\,\psi'(\lambda^3)&\left((\mathrm{tr}\,\mathbf{L})\mathbf{M} - (\mathrm{tr}\,\mathbf{M})\mathbf{L}\right)\cdot(\mathbf{n}_0\otimes\mathbf{n}_0)\\ &+ \psi(\lambda^3)\left(\mathbf{LM} - \mathbf{ML}\right)\cdot(\mathbf{n}_0\otimes\mathbf{n}_0) = 0.\end{aligned} \tag{A.4}$$

The constitutive map φ – and hence π – drops out of (A.4), as expected. We now pick $\mathbf{L} = \mathbf{M}^\top = \mathbf{n}_0\otimes\mathbf{m}$, with $\mathbf{m}$ a unit vector orthogonal to $\mathbf{n}_0$: $|\mathbf{m}| = 1$ & $\mathbf{m}\cdot\mathbf{n}_0 = 0$, i.e., two simple shears in the plane spanned by $\{\mathbf{m},\mathbf{n}_0\}$, $\mathbf{L}$ along $\mathbf{n}_0$ and $\mathbf{M}$ along $\mathbf{m}$. Since both are traceless and their two products are respectively equal and orthogonal to $\mathbf{n}_0\otimes\mathbf{n}_0$, (A.4) boils down to

$$\psi(\lambda^3) = 0 \text{ for all } \lambda > 0 \iff \alpha = 0. \tag{A.5}$$

That $\alpha = 0$ is also sufficient for hyperelasticity is obvious.

B   Nematic hyperelasticity, old and new

In all part $\mathscr{P}$ of a hyperelastic body the power expended equals the time derivative of the stored energy:

$$\int_{\mathscr{P}} \mathbf{T}\cdot(\boldsymbol{\nabla}\mathbf{v})\,dV = \int_{\mathscr{P}} (\rho\,\sigma\,dV)^{\cdot}, \tag{B.1}$$

where $\mathbf{T}$ is the Cauchy stress, $\mathbf{v}$ the spatial velocity field, ρ the current mass density, σ the stored energy density with respect to mass, and the integration is done with respect to the *current* volume. Since $J := \det\mathbf{F} = dV/dV_0$ and the reference volume V_0 does not depend on time, equality (B.1) translates into

$$\int_{\mathscr{P}} \left(J\mathbf{T}\mathbf{F}^{-\top}\right)\cdot\dot{\mathbf{F}}\,dV_0 = \int_{\mathscr{P}} (J\rho\,\sigma)^{\cdot}\,dV_0, \tag{B.2}$$

where use has been made of the differential relation linking the spatial velocity field with the deformation gradient: $\boldsymbol{\nabla}\mathbf{v} = \dot{\mathbf{F}}\mathbf{F}^{-1}$. Mass conservation implies $(J\rho)^{\cdot} = 0$. Hence, (B.2) localises into

$$\mathbf{S}\cdot\dot{\mathbf{F}} = \rho_0\,\dot{\sigma}, \tag{B.3}$$

where $\rho_0 = J\rho$ is the reference mass density and

$$\mathbf{S} := J\mathbf{T}\mathbf{F}^{-\top} \tag{B.4}$$

is the Piola stress. Since $\dot{\sigma} = (\partial\sigma/\partial\mathbf{F})\cdot\dot{\mathbf{F}}$, a necessary and sufficient condition for (B.1) to be satisfied along all motions is that

$$\mathbf{S} = \rho_0\,\frac{\partial\sigma}{\partial\mathbf{F}}. \tag{B.5}$$

On this basis, we now consider the specific constitutive assumption (13)–(14) and, using (54), compute the derivatives

$$\frac{\partial\sigma_{\texttt{iso}}}{\partial\mathbf{F}} = -\rho\,\sigma'_{\texttt{iso}}\mathbf{F}^{-\top}, \tag{B.6a}$$

$$\frac{\partial(\boldsymbol{\Psi}^{-1}\cdot\mathring{\mathbf{B}})}{\partial\mathbf{F}} = 2\,\mathrm{dev}(\boldsymbol{\Psi}^{-1}\,\mathring{\mathbf{B}})\,\mathbf{F}^{-\top} \tag{B.6b}$$

$$-\tfrac{3}{2}(a'/a)(\rho/J)\,\mathrm{dev}(\mathbf{n}_0\otimes\mathbf{n}_0)\cdot(\boldsymbol{\Psi}^{-1}\,\mathring{\mathbf{B}})\,\mathbf{F}^{-\top}.$$

Summing up all contributions to (B.5) and inverting (B.4) – i.e., calculating $\mathbf{T} = J^{-1}\mathbf{S}\mathbf{F}^\top$ – yields (15)–(16).

To extend the theory founded on (13)–(14) to cover the case when the constraint on the nematic texture is lifted and the director is set free to rotate, the stored energy density should be augmented (at least) as follows [21]:

$$\sigma_+(\mathbf{F},\mathbf{n},\nabla\mathbf{n}) = \hat{\sigma}(\rho,\mathbf{n},\mathring{\mathbf{B}}) + \sigma_{\mathrm{OF}}(\rho,\mathbf{n},\nabla\mathbf{n}), \tag{B.7}$$

with σ_{OF} the Oseen-Frank free-energy density function.

The study of small-amplitude plane waves as done in Secs. 2.4 and 3.2 only depends on the *linearised* features of the theory. Therefore we find it appropriate to provide an explicit expression of the free-energy density function (13)–(14) – specialised to a slightly compressible anisotropic fluid as defined in Sec. 2.3 – when truncated after $O(\varepsilon^2)$ terms, with ε the smallness parameter reducing the amplitude of the displacement field $\mathbf{u}$ in (32a).

Let $\mathbf{F} = \mathbf{I} + \varepsilon\nabla\mathbf{u}$. Then, the Taylor expansion of the determinant close to the identity yields

$$J = \det\mathbf{F} = \det(\mathbf{I} + \varepsilon\nabla\mathbf{u}) \tag{B.8}$$
$$= 1 + \varepsilon\,\mathrm{tr}\nabla\mathbf{u} + \tfrac{1}{2}\varepsilon^2\big((\mathrm{tr}\nabla\mathbf{u})^2 - \mathrm{tr}((\nabla\mathbf{u})^2)\big) + o(\varepsilon^2)$$
$$= 1 + \varepsilon\,\mathrm{tr}\mathbf{E} + \tfrac{1}{2}\varepsilon^2\big((\mathrm{tr}\mathbf{E})^2 - (\nabla\mathbf{u})\cdot(\nabla\mathbf{u}^\top)\big) + o(\varepsilon^2),$$

where $\mathbf{E} := \mathrm{sym}\nabla\mathbf{u}$ is the infinitesimal deformation. Notably, the differential identity [40]

$$(\nabla\mathbf{u})\cdot(\nabla\mathbf{u}^\top) = \mathrm{div}\big((\nabla\mathbf{u})\mathbf{u} - (\mathrm{div}\,\mathbf{u})\mathbf{u}\big) + (\mathrm{tr}\mathbf{E})^2 \tag{B.9}$$

cancels all second-order terms in (B.8) to within the *null Lagrangian* $-\varepsilon^2 n$, with

$$n := \tfrac{1}{2}\,\mathrm{div}\big((\nabla\mathbf{u})\mathbf{u} - (\mathrm{div}\,\mathbf{u})\mathbf{u}\big). \tag{B.10}$$

Therefore, the scaled density variation (23) expands as

$$\xi = J^{-1} - 1 = -\varepsilon\,\mathrm{tr}\mathbf{E} + \varepsilon^2(\mathrm{tr}\mathbf{E})^2 + \varepsilon^2 n + o(\varepsilon^2). \tag{B.11}$$

Finally, on account of (24), (25) and (26), the contribution of the isotropic term σ_{iso} to the elastic energy *per unit reference volume* reads

$$\rho_0\sigma_{\mathrm{iso}} = -\varepsilon\,p_0\,\mathrm{tr}\mathbf{E} + \tfrac{1}{2}\varepsilon^2\rho_0 p_1(\mathrm{tr}\mathbf{E})^2 + o(\varepsilon^2), \tag{B.12}$$

after pruning the ineffective terms, namely, the constant $\rho_0\sigma_{\mathrm{iso}}(\rho_0)$ and the null Lagrangian $\varepsilon^2 p_0 n$. Also the contribution of the equilibrium pressure p_0 to the second-order term has been dropped, being negligible compared to that of $\rho_0 p_1$ (cf. (26)).

The isochoric component of the deformation gradient reads

$$\mathring{\mathbf{F}} = J^{-1/3}\mathbf{F} = \mathbf{I} + \varepsilon\mathbf{D}$$
$$\quad - \tfrac{1}{3}\varepsilon^2\Big((\mathrm{tr}\mathbf{E})\mathbf{D} + \tfrac{1}{6}(\mathrm{tr}\mathbf{E})^2\mathbf{I} + \tfrac{1}{2}(\boldsymbol{\Theta}\cdot\boldsymbol{\Theta} - \mathbf{E}\cdot\mathbf{E})\mathbf{I}\Big) + o(\varepsilon^2), \tag{B.13}$$

where

$$\boldsymbol{\Theta} := \mathrm{skw}\nabla\mathbf{u}, \quad \mathbf{D} := \mathrm{dev}\nabla\mathbf{u} = \mathrm{dev}\mathbf{E} + \boldsymbol{\Theta}, \tag{B.14}$$

with $\mathrm{skw}\nabla\mathbf{u}$ the skew-symmetric part of $\nabla\mathbf{u}$. The left Cauchy-Green strain tensor associated with $\mathring{\mathbf{F}}$ is

$$\mathring{\mathbf{B}} = \mathring{\mathbf{F}}\mathring{\mathbf{F}}^\top = \mathbf{I} + 2\varepsilon\,\mathrm{dev}\mathbf{E}$$
$$+ \varepsilon^2\Big(-\tfrac{2}{3}(\mathrm{tr}\mathbf{E})\,\mathrm{dev}\mathbf{E} - \tfrac{1}{9}(\mathrm{tr}\mathbf{E})^2\mathbf{I} + \tfrac{1}{3}(\mathbf{E}\cdot\mathbf{E} - \boldsymbol{\Theta}\cdot\boldsymbol{\Theta})\mathbf{I} \tag{B.15}$$
$$+ (\mathrm{dev}\mathbf{E} + \boldsymbol{\Theta})(\mathrm{dev}\mathbf{E} - \boldsymbol{\Theta})\Big) + o(\varepsilon^2).$$

We now expand the inverse of the shape tensor (14) by using (B.11) and (27) extended to second order:

$$a = 1 + a_0 + a_1\xi + \tfrac{1}{2}a_2\xi^2 + o(\xi^2). \tag{B.16}$$

As in Secs. 2.4 and 3.2, we will neglect terms of order $O(a_0)$, seen to be insignificant (cf. the last paragraph of Sec. 2.4), obtaining

$$\boldsymbol{\Psi}^{-1} = \mathbf{I} - 3a_1\xi\,\mathrm{dev}(\mathbf{n}_0\otimes\mathbf{n}_0) + 3a_1^2\xi^2\mathbf{n}_0\otimes\mathbf{n}_0$$
$$- \tfrac{3}{2}a_2\xi^2\,\mathrm{dev}(\mathbf{n}_0\otimes\mathbf{n}_0) + o(\xi^2)$$
$$= \mathbf{I} + 3\varepsilon a_1(\mathrm{tr}\mathbf{E})\,\mathrm{dev}(\mathbf{n}_0\otimes\mathbf{n}_0) + 3\varepsilon^2 a_1^2(\mathrm{tr}\mathbf{E})^2\mathbf{n}_0\otimes\mathbf{n}_0 \tag{B.17}$$
$$- 3\varepsilon^2\big(a_1 n + (a_1 + \tfrac{1}{2}a_2)(\mathrm{tr}\mathbf{E})^2\big)\mathrm{dev}(\mathbf{n}_0\otimes\mathbf{n}_0) + o(\varepsilon^2).$$

From (B.15) and (B.17) we finally get the contribution of the anisotropic term in (13) to the elastic energy per unit reference volume:

$$\tfrac{1}{2}\rho_0\mu\,\mathrm{tr}\big(\boldsymbol{\Psi}^{-1}\mathring{\mathbf{B}} - \mathbf{I}\big) = \rho_0\mu_0\varepsilon^2\Big((\mathrm{dev}\mathbf{E})\cdot(\mathrm{dev}\mathbf{E})$$
$$+ \tfrac{9}{2}a_1^2(\mathrm{tr}\mathbf{E})^2 + 3a_1(\mathrm{tr}\mathbf{E})(\mathrm{dev}\mathbf{E})\cdot(\mathbf{n}_0\otimes\mathbf{n}_0)\Big) + o(\varepsilon^2). \tag{B.18}$$

Note that all the second-order terms in $\boldsymbol{\Psi}^{-1}\mathring{\mathbf{B}} - \mathbf{I}$ affected by either the null Lagrangian n or the infinitesimal rotation $\boldsymbol{\Theta}$ or the second-order coefficient of the asphericity factor a_2 are traceless and hence disappear from (B.18).

At this point it is appropriate to consider the quadratic free energy surmised by Mullen, Lüthi and Stephen [10], which we alluded to in Sec. 1: 'The experimental anisotropy in the sound velocity ...can be explained if at [finite] frequencies a liquid crystal in some respects behaves like a solid and the free energy contains terms like

$$F = \tfrac{1}{2}k_1(u_{xx} + u_{yy})^2 + k_2(u_{xx} + u_{yy})u_{zz} + \tfrac{1}{2}k_3 u_{zz}^2, \tag{B.19}$$

where the k's are elastic constants, and the u_{ij} are the elastic strains. We have chosen the z axis to be along the director.' Translated into our component-free notation, (B.19) reads

$$F = \tfrac{1}{2}k_1(\mathrm{tr}_\perp\mathbf{E})^2 + k_2(\mathrm{tr}_\perp\mathbf{E})\varepsilon_{\mathbf{n}} + \tfrac{1}{2}k_3\varepsilon_{\mathbf{n}}^2, \tag{B.20}$$

with

$$\varepsilon_{\mathbf{n}} := \mathbf{E}\cdot(\mathbf{n}_0\otimes\mathbf{n}_0), \quad \mathrm{tr}_\perp\mathbf{E} := \mathrm{tr}\mathbf{E} - \varepsilon_{\mathbf{n}}. \tag{B.21}$$

On the other hand, the sum of the quadratic terms in (B.12) and (B.18) involving the trace of $\mathbf{E}$ may be reorganised as follows:

$$\tfrac{1}{2}\rho_0 p_1\big(1 + \eta a_1(9a_1 - 2)\big)(\mathrm{tr}_\perp\mathbf{E})^2 +$$
$$\rho_0 p_1\big(1 + \eta a_1(9a_1 + 1)\big)(\mathrm{tr}_\perp\mathbf{E})\varepsilon_{\mathbf{n}} + \tag{B.22}$$
$$\tfrac{1}{2}\rho_0 p_1\big(1 + \eta a_1(9a_1 + 4)\big)\varepsilon_{\mathbf{n}}^2$$

where η is the small parameter introduced in (31). Therefore, we identify the elastic constants in (B.19) as small perturbations of the bulk modulus $\rho_0 p_1$, parametrised by the product of the shear modulus $\rho_0\mu_0$ and the sensitivity coefficient a_1. What matters is the slight differences between them, namely,

$$k_3 - k_2 = k_2 - k_1 = 3\rho_0\mu_0 a_1 + o(\eta). \tag{B.23}$$

Note that (B.23) implies $k_2^2 = k_1 k_3 + o(\eta)$, a condition – postulated in Ref. 10 – that eliminates propagating shear modes at order $O(\eta)$. However, (B.18) contains also a term quadratic in $\mathrm{dev}\mathbf{E}$ of order $O(\eta)$, which sustains such waves.

Title: Anisotropic wave propagation in nematic liquid crystals
Authors: Paolo Biscari, Antonio DiCarlo, and Stefano S. Turzi
Journal: *Soft Matter*
Ms. Ref. No.: SM-ART-05-2014-001067
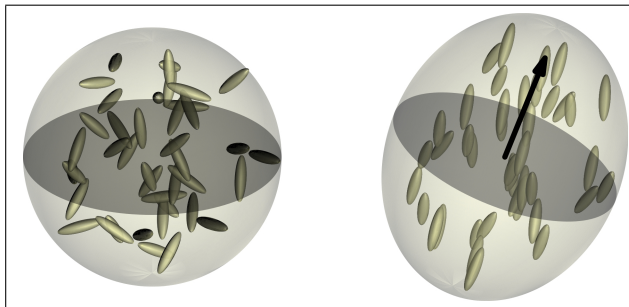
We show that elastic anisotropy and relaxation are at the origin of the main experimental features of nematoacoustics.